The challenge of shot-noise limited speckle patterns statistical analysis

J.-M. Tualle, K. Barjean, E. Tinet, D. Ettori

Laboratoire de Physique des Lasers, CNRS UMR 7538, Université Paris 13, Institut Galilée, 99 Ave J.B. Clément, F-93430 Villetaneuse, France

Abstract

We propose to analyze in details the performances of an ASIC dedicated to the real-time analysis of speckle patterns statistics. This IC calculates average statistical values over the whole pixel array, and outputs only these values instead of a whole image: such on-chip calculation achieves the high acquisition rates required to follow speckle patterns from thick living tissue, without additional noises usually associated with fast data transfer. We want to assess if our device can reach its shot-noise limit, which is the shot-noise limit on one pixel divided by the square root of the number of pixels.

Introduction

The real-time statistical analysis of speckle patterns is a generic technological bottleneck for biomedical optics, when diffuse light is under consideration. It covers different applications from time-resolved diffuse correlation spectroscopy in thick media [1,2] to acousto-optic imaging, where the coupling of diffuse light with an ultrasound beam induces oscillations of the speckle pattern: filtering of these oscillations allows 3D imaging in optically turbid media with the spatial resolution of ultrasounds [3].

Of course, speckle analysis suffers from the low spatial coherence of speckle patterns: there is no incentive to take detectors bigger than a coherence area (the speckle "grain" size) for recording speckle fluctuations. In fact, multi-pixels detectors should be a good tool for such a task, as the signal to noise ratio (SNR) increases with the number of detectors. We already presented a bi-dimensional pixel CMOS detector array specifically designed for this task [4,5], with parallel in-pixel demodulation and time-resolved correlation computation. The calculation of such averaged values of the whole pixels array is a main feature of this architecture, and allows us to reach high frame rates (higher than 10,000 frames/s) compatible with the fast decorrelation expected in living biological tissue. However, one has to check if it allows reaching optimal performance, with shot noise limited measurements.

We propose to explore this question in details, with an assessment of measurements at both the pixel and the pixel array levels. Indeed, even if the shot-noise level is reached at the pixel level, at the pixel array level the SNR should be multiplied by the square root of the number of pixels, what is a more stringent constraint. Some really low noises, spatially correlated on a high number of pixels, could indeed have a great contribution, preventing optimal performances. These noises may originate from the low frequency noise of bias voltages or, on the contrary, from high frequency parasitic events due to the digital resources used in the protocol. Furthermore, a non-uniformity of pixels' gain could also

deteriorate the SNR. These factors will be quantitatively assessed, and different ways to overcome these difficulties will be proposed.

IC Architecture and Functionalities

The architecture of the CMOS sensor considered in this paper is summarized on figure 1. The photo-current is multiplied by a demodulation signal after rejection of the DC component. The multiplication structure is made of two NMOS transistors M2 and M3 working in the weak inversion linear regime [4]. The multiplied signal is then integrated, leading to a lock-in measurement representative of the speckle grain properties. This lock-in signal is stored in a 9-registers analog memory, and a four-quadrant multiplier architecture [6] (MULT in figure 1) makes it possible to compute either the square of the lock-in signal, or a temporal correlation through the multiplication of two different registers. These quantities have the advantage to present a non-zero average despite spatial incoherence of speckle patterns, and it is worth outputting only values averaged over the whole pixel array. A main feature of the four-quadrant multiplier is the fact that it outputs currents, so that the average of whole pixels can be implemented in a very simple way, summing all these currents with Kirchhoff's point rule.
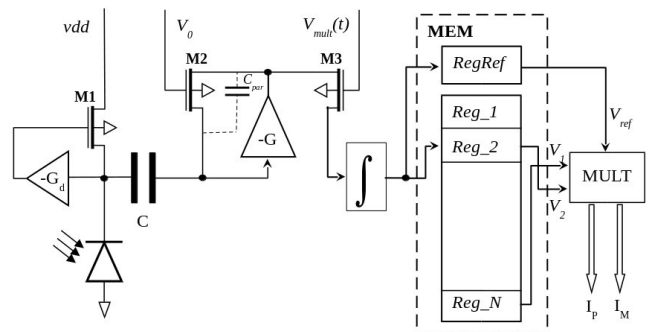
Figure 1. CMOS sensor for speckle patterns analysis: Block diagram for one pixel.

This IC was already tested in different setups in the field of biomedical optics [7,8], but the most accurate way for performances assessment is analyze a weakly-modulated laser beam. The figure 2 presents the lock-in signal measured from a laser beam with a 500kHz modulation. At the pixel level, the laser beam induces a photocurrent with a DC component estimated at 1nA from the direct measurement of the photodiode bias current. The amplitude of the modulated photocurrent can then be easily

deduced, and it is estimated at 25pA. Let us note that this IC was designed for interferometric measurements [7,8], and that the simple detection of a modulated signal is not such a measurement, but it is still a good model. Interferences between two electromagnetic fields will indeed give rise to a photocurrent which can be expressed as:

$$i_{ph}(t) = 2\sqrt{i_0 i_1}\cos(2\pi f t + \phi) \qquad (1)$$

where is i_0 the photocurrent corresponding the reference beam, and where i_1 corresponds to the optical signal. If T is the integral duration, the optical signal corresponds to $n = T\, i_1\, /e$ photo-electrons, and the modulation (1) can be rewritten

$$i_{ph}(t) = 2\delta i \sqrt{n}\cos(2\pi f t + \phi) \qquad (2)$$

With

$$\delta i = \sqrt{\frac{e i_0}{T}} \qquad (3)$$
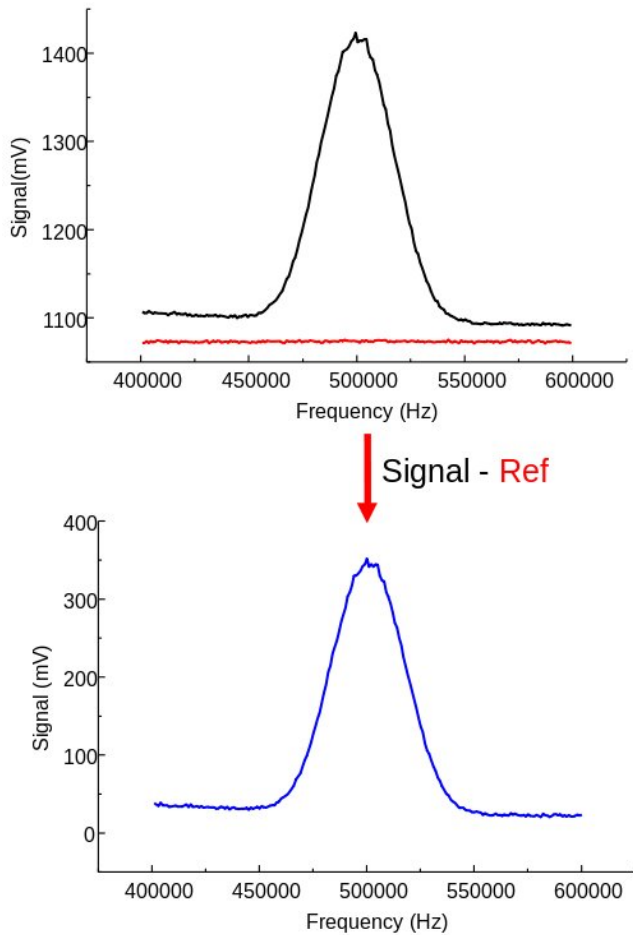
Figure 2. Lock-in signal recorded by the IC from a 500kHz weakly-modulated laser beam.

Inserting experimental values for these parameters, with T=50µs in this experiment and i_0 = 1nA, we deduce that a DC amplitude of 25pA is a model for an interferometric experiment with 50 photo-electrons in the signal beam.

The signal recorded by the IC (black curve on figure 2) has an arbitrary offset, and reference measurements are without any demodulation signal (red curve) in order to remove this offset (blue curve). There is still an offset after the subtraction of reference measurements, and the height of the lock-in peak corresponds to 320mV with respect to this residual offset. The origin of this offset and the consistence of the peak value will be analyzed in next section. Let us present in figure 3 a bode diagram of this peak value as a function of the signal frequency. In this exemple we obtained a cutoff frequency of 1MHz.

The sensor cutoff frequency depends of course on its gain, which is fixed by the transimpedance of transistor M2 (4GΩ in the present experiment), and by the properties of the amplifier used in the lock-in multiplier structure (gain -G, with a gain-bandwidth product of ~10GHz). One should expect a ~5MHz bandwidth from these values, but results are in fact dramatically affected by the drain-source parasitic capacitance of M2: we estimated from simulations that a 20aF capacitance should explain experimental results.
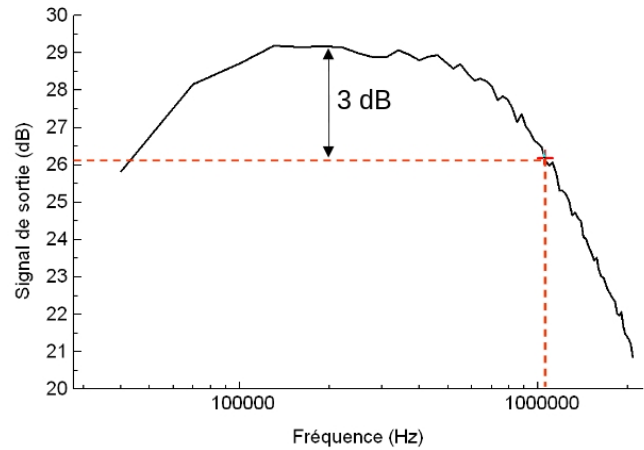
Figure 3. Experimental Bode diagram extracted from the lock-in peak measured at different signal frequencies.

A last feature of the IC is its capability to compute temporal correlations. This can be illustrated by the introduction of a phase-shift Δφ between the laser modulation and the demodulation signal, and to multiply lock-in components respectively taken with and without this phase-shift, what should lead to a cos(Δφ) dependance [4]. The figure 4 presents some results obtained for Δφ=0 (no correlation, black curve), Δφ=π/2 (uncorrelated signal, red curve), Δφ=π (anticorrelation, blue curve), Δφ=3π/2 (uncorrelated, pink curve). The ability of the IC to quantify correlation properties of speckle pattern has already been confirmed [7].
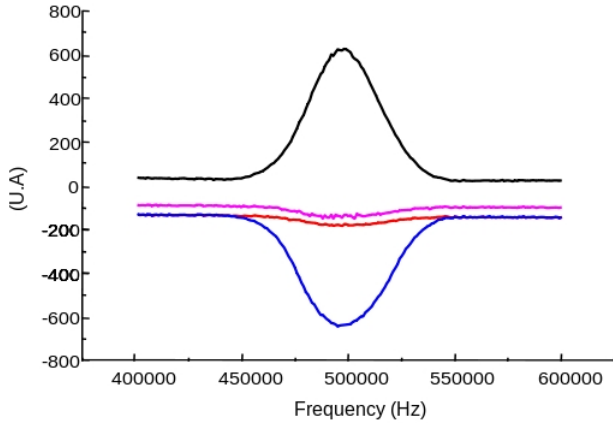
Figure 4. Correlation signals taken for different values of the phase-shift $\Delta\varphi$ between the laser modulation and the demodulation signal.

Assessment of the measured signal

The integration system is not an ideal one, and in fact the integrator voltage satisfies the equation:

$$\frac{ds}{dt} + \frac{\xi(t)}{AR_2C_i}s = \frac{1}{C_i}\xi(t)i(t) \tag{4}$$

In equation (4), the term $\xi(t)$ is the ratio between the transimpedances of transistors M2 and M3, and corresponds to the demodulation function. Strictly speaking, one has:

$$\xi(t) = g[f_0(t) + f_{mul}(t)] \tag{5}$$

where $f_{mul}(t)$ is a demodulation function, whereas $f_0(t)$ is a slowly varying function which ensures the positivity of $\xi(t)$. The factor g in equation 5 is the gain of the lock-in system, C_i is the integrator capacitance, A is the gain of the integrator amplifier, and R_2 is the transimpedance of transistor M2. Let us note that the current $i(t)$ in equation (4) is not exactly the photocurrent: the capacity C of the low-pass filter in figure 1 indeed forms a voltage divider with the internal capacitance of the photodiode, so that we have $i(t)=\gamma \cdot i_{ph}(t)$, with $\gamma=0.26$. Taking this fact into account, it appears that the solution of equation (4) with the photocurrent of equation (2) reads:

$$S_i = \lambda g \gamma \frac{\delta i}{C_i} T \sqrt{n} \cos\phi \tag{6}$$

where ϕ is a random phase (no synchronisation between the laser modulation and the demodulation signal), and where

$$\lambda = \frac{1}{T}\int_0^T exp\left[-\int_t^T \frac{f_0(t\prime)}{AR_2C_i}dt'\right]dt \tag{7}$$

Introducing the gain K of the four-quadrant multiplier, we then have for the phase-averaged squared signal:

$$\langle S_i{}^2\rangle = \frac{K}{2}\left(\lambda g\gamma \frac{\delta i}{C_i}T\right)^2 n \equiv X_0 n \tag{8}$$

The numerical value of this expression depends on the gain g and its ability to optimize the product λg . In the experiment, the transimpedance of the transistor M3 was set in order to get an optimal value of 5.6 for this product. We finally obtain a value of 15mV for X_0 , so that a value of 750mV is expected for the peak signal (figure 2) with a photocurrent modulation of 25pA. In figure 5, we plot the experimental value of the signal taken at 500kHz and 25pA for different powers of the laser beam, *i.e.* for different values of the DC part i_0 of the photocurrent. No value for i_0 lower than 0.5nA is reported in this figure due to the difficulty to warrant a 25pA with our modulation system in that case. Anyway, it appears on figure 5 that the measured peak value is close to 750mV for small values of i_0 , and that the lower value recorded on figure 2 is related to some saturation effect observed when i_0 increases.

The origin of this saturation has to be questioned as the DC part is filtered, so that i_0 should have no effect. In fact, noises linked to this current, and more specifically the shot-noise, increase with i_0 and lead to a saturation of transistors M2 and M3 of the lock-in detection. Such a phenomenon appears to be a first limitation of this architecture.
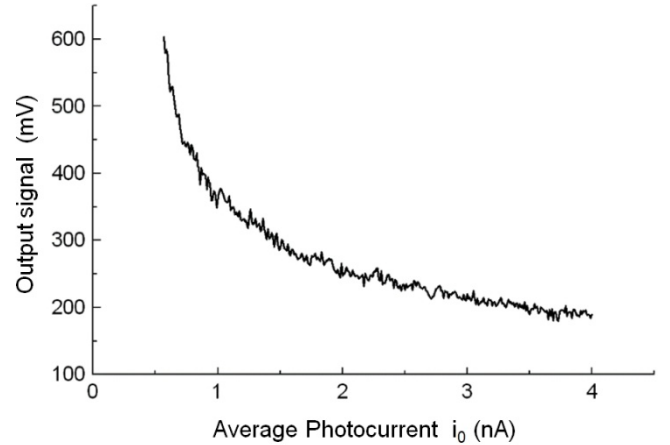
Figure 5. Peak value observed with a 25pA modulation of the photocurrent at 500kHz, as a function of the DC photocurrent i_0.

Variance of the noise

Let us now consider the presence of a noise i_b, in the absence of any signal for the sake of clarity. Using the same steps as for equation (6), let us write the solution of equation (4) as:

$$S_b = \frac{g}{C_i}\int_0^T exp\left[-\int_t^T \frac{gf_0(t')}{AR_2C_i}dt'\right]f_{mul}(t)i_b(t)dt \tag{9}$$

To derive this expression, we used the fact that the DC part of the photocurrent noise is filtered, so that $f_0(t)i_b(t)$ cancels in average. The average value of S_b^2 can then be easily derived assuming that i_b is a white noise. Considering shot-noise, which is a fundamental physical limitation in this experiment, one can indeed write:

$$\langle i_b(t)i_b(t')\rangle = 2\gamma^2 e\, i_0\, \delta(t-t') \tag{10}$$

In this expression, the factor 2 account both for the photocurrent shot-noise and for the shot-noise of the biasing transistor M1 (see figure 1). This leads, for the variance of S_b , to:

$$\langle S_b^2 \rangle = \lambda' \left(\gamma \delta i \frac{g}{C_i} T \right)^2 \tag{11}$$

with

$$\lambda' = \frac{1}{T} \int_0^T \exp \left[-2 \int_t^T \frac{g f_0(t')}{AR_2 C_i} dt' \right] f_0^2(t) dt \tag{12}$$

The noise therefore has a non-zero variance, and this will contribute to the measured signal as an offset, as observed on figure 2. Introducing the gain K of the four-quadrant multiplier and the parameter X_0 introduced in equation (8), one has:

$$X_b \equiv K \langle S_b^2 \rangle = \frac{2\lambda'}{\lambda^2} X_0 \propto i_0 \tag{13}$$

We found $2\lambda'/\lambda^2 \sim 1.95$, leading to a value of 58mV for X_b at $i_0 = 1$nA. We recorded the evolution of this offset with measurements performed in the same way as for figure 2, but in the absence of signal. These results are presented as a function of i_0 in figure 6. A small residual constant offset of about 20mV was manually removed so that the curve passes through the origin.
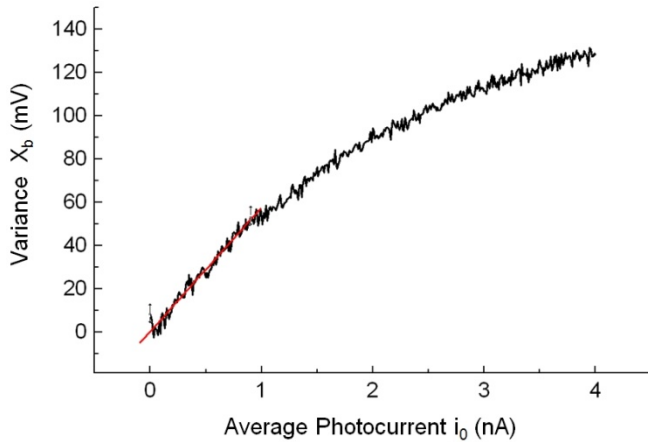
Figure 6. Evolution of the signal offset as a function of i_0. According to the theory, this corresponds to the variance of the shot-noise.

It appears that the value measured for X_b at $i_0 = 1$nA fits well with the theoretical estimation, as the linear behavior observed for small values of i_0. There is however saturation clearly visible at higher values. We could expect that this saturation has the same origin as the saturation observed for the signal in figure 5. This leads us to compute the ratio between those curves in order to remove this effect. We plot on figure 7 the ratio of the variance X_b over the signal, and observe a clear linear behavior, as expected for X_b in equation (13). Of course, as the value of 320mV of the signal at $i_0 = 1$nA is lower than the expected one, while the value of X_b corresponds to the expected one, the slope of the linear behavior in figure 7 is higher than expected. The SNR is therefore lower than expected by a factor 2.25: a noise factor of about 2.25 therefore appears due to the saturation effect in the lock-in detection.
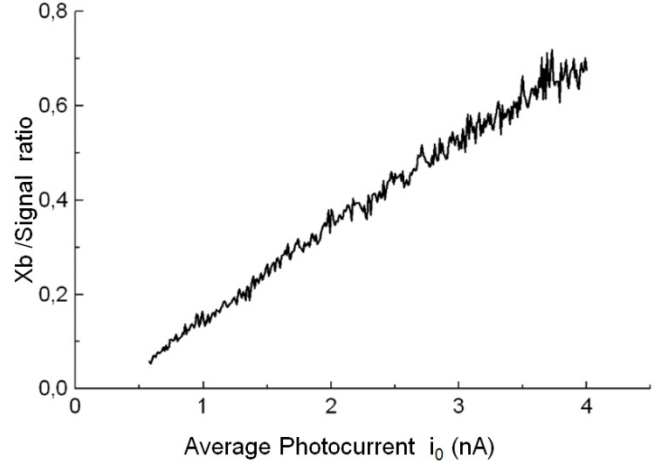
Figure 7. Ratio figure 6/ Figure 5

Average over the pixel array

The main feature of the IC is to perform an average of pixel values over the whole pixel array. In fact, the IC simply estimates the sum of the pixels. At this stage, we can account for pixels non-uniformity through the introduction of a gain G_i for each pixel which should represent the ratio between the observed value and the ideal one:

$$X = \sum G_i x_i \tag{14}$$

One has for the average of this expression:

$$\langle X \rangle = (\sum G_i) \langle x_i \rangle \tag{15}$$

where N is the pixel number. In the same way, one has for its variance:

$$Var_X = (\sum G_i^2) \langle Var_x \rangle \tag{16}$$

And the SNR evolves as:

$$SNR_X = \sqrt{\frac{\langle X \rangle^2}{Var_X}} = \sqrt{\frac{(\sum G_i)^2}{\sum G_i^2}} SNR_x \equiv \sqrt{N_{eff}} \; SNR_x \tag{17}$$

For ideal pixels, with $G_i = 1$, one has $N_{eff} = N$, the pixel number, and we recover that the SNR over the whole array is equal to the SNR for one pixel increased by the square root of the pixel number. In case of non-uniform pixels, one can use this result in equation (17), but with an effective pixel number N_{eff} . The IC is a 24x24 pixels test microchip: we measured the gain of each pixel independently, and found an effective pixel number of ~300 instead of 576 [9].

Let us now insist on the fact that the variance X_b in equation (3) is the variance of the noise at the pixel level, but before the four-quadrant multiplier. Assuming a Gaussian noise, the variance of the noise after this multiplication is

$$\langle S_b^4 \rangle = 2 \langle S_b^2 \rangle^2 \tag{18}$$

So, if there were one pixel, the standard deviation of the noise in the output would be $\sqrt{2}\,X_b$. This has to be divided by $\sqrt{N_{eff}}$ in order to estimate the output noise. To finish with, the results presented in figure 2 are averaged over 900 measurements. Finally, one also has to account for the subtraction of reference measurements (red curve of figure 2) through an additional $\sqrt{2}$ factor, so that the expected noise in this figure is:

$$\frac{\sqrt{2}X_b}{\sqrt{900N_{eff}}} = 0.3mV \qquad (19)$$

In order to check this value, let us focus on the wings of the lock-in response, corresponding to the 400-450kHz range in figure 2.
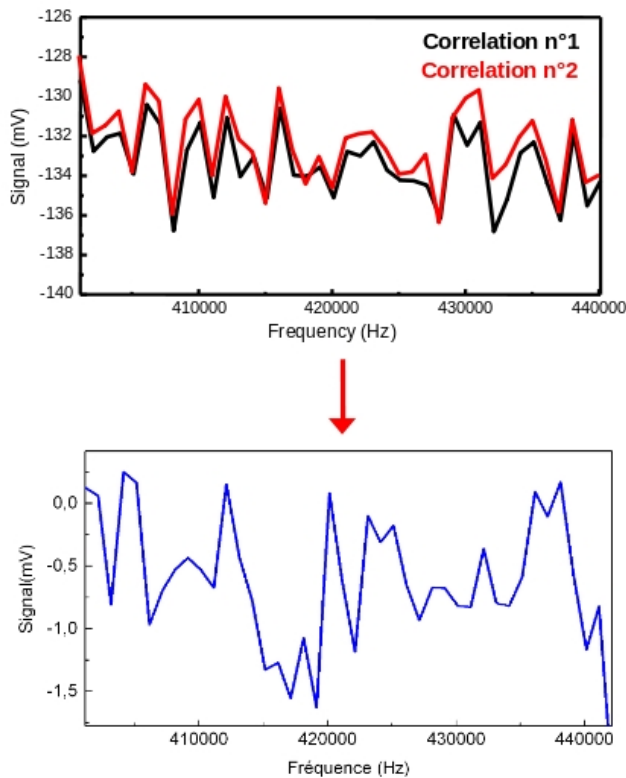
Figure 8. Noise on the wings of the lock-in response, for two different correlation measurements (black and red): the correlated noise can be removed in the difference of these signals (blue).

The noise on the black curve of figure 8 has a standard deviation of 1.5mV, that is 5 times more than expected. This represents another difficulty, linked to the fact than the law in equation (17) is satisfied only with spatially uncorrelated noises. Using measurements performed on each pixel independently, we indeed proved that this noise comes from a small noise perfectly correlated over all pixels [9]. We suspect that this noise comes from low frequency fluctuations of the bias voltages: indeed, the correlation measured exactly at the same time (red curve of figure 8) presents almost the same fluctuations. As these curves correspond to different signals (see for instance figure 3), it is legitimate to perform their difference: this is performed on figure 8, and the resulting noise is 0.4mV, what is plainly

compatible with the expected noise after the introduction of an additional $\sqrt{2}$ factor to account for the signal difference.

Conclusion and Perspectives

In conclusion we have exposed the two main limitations in the IC architecture proposed for the real-time analysis of the speckle patterns:

- The shot-noise limit is not fully reached at the pixel level due to a saturation of the lock-in detection system by this noise. A 2.25 factor is lost due to this phenomenon;
- Spatial non-uniformity of the pixel array do not allow a full exploitation of the pixel number: we observed an effective pixel number of 300 instead of 24x24=576, what means a reduction of the SNR by a factor of about 1.4 .
- Noises correlated over a large set of pixels can considerably deteriorate the SNR. We can overcome this with convenient differences. Therefore, it's not too problematic for applications related to correlation measurement.

These results are still not completely satisfying, and prevent us to launch the design of a larger IC with a very large number of pixels. Some work is still needed to circumvent these issue.

Funding

References

[1] J.-M. Tualle, H.L. Nghiem, M. Cheikh, D. Ettori, E. Tinet and S. Avrillier, "Time-Resolved Diffusing Wave Spectroscopy for selected photon paths beyond 300 transport mean free paths", Journal of the Optical Society of America A, vol. 23, no. 6, pp. 1452-1457, 2006.

[2] M. Cheikh, H.L Nghiem, D. Ettori, E. Tinet, S. Avrillier, J.M. Tualle, "Time-resolved diffusing wave spectroscopy applied to dynamic heterogeneity imaging", Optics letters, vol. 31, no. 15, pp. 2311-2313, 2006.

[3] S. Farahi, E. Benoit, A. Grabar, J,-P, Huignard, and F. Ramaz, "Time resolved three-dimensional acousto-optic imaging of thick scattering media", Optics Letters, vol. 37, no. 13, pp. 2754-2756, 2012.

[4] J.-M. Tualle , A. Dupret, M. Vasiliu, "Ultra-compact sensor for diffuse correlation spectroscopy", Electronics Letters vol. 46, n. 12, pp. 819-820, 2010.

[5] K. Barjean, D. Ettori, E. Tinet, A. Dupret, J.-M. Tualle, "An ultra fast, ultra compact sensor for diffuse wave spectroscopy", Proceedings of SPIE – Vol. 8659, Sensors, Cameras, and Systems for Industrial/Scientific Applications XIV, 865906, 2013.

[6] G. Han, E. Sanchez-Sinencio, "CMOS transconductance multipliers: a tutorial", IEEE Transactions on Circuits and Systems II: Analog and Digital Signal Processing., vol. 45, no. 12, pp. 1550-63., 1998.

[7] J.-M. Tualle, K. Barjean, É. Tinet, D. Ettori, "High sensitivity analysis of speckle patterns: a technological challenge for biomedical optics", Proceedings of SPIE – Vol. 8659, Sensors, Cameras, and Systems for Industrial/Scientific Applications XIV, 86590K, 2013.

[8] K. Barjean, K. Contreras, J.-B. Laudereau, É. Tinet, D. Ettori, F Ramaz, and J.-M. Tualle, "Fourier transform acousto-optic imaging with a custom-designed CMOS smart-pixels array", Optics Letters, Vol. 40, no. 5, pp. 705-708, pp, 2015.

[9] K. Barjean, PhD thesis, 2015.

Author Biography

Jean-Michel Tualle is working in the biomedical optics group, at the Paris 13 University, on light propagation in turbid media and tissue characterization for medical diagnosis. He notably proposed a new method to perform time-resolved measurements of diffuse light, using the heterodyne fluctuations of a speckle interferogram induced by a wavelength-modulated source. Following this work, he was led to be interested to smart-pixels array sensors, which are suitable for real-time analysis of speckle patterns. He designed, in collaboration with Institut d'Electronique Fondamentale (Orsay), a dedicated IC for the analysis of speckle interferograms which is now considered for applications in acousto-optics imaging. He signs 35 publications, 51 conferences, and is co-inventor of three patents. He is member of the program committee of the SPIE conference Electronic Imaging: Image Sensors and Imaging Systems. He is co-organizing the OptDiag national congresses since 2007 (http://optdiag2016.univ-paris13.fr/).